

Atmospheric Neutrinos ^{*)}

Morihiro HONDA¹, Takaaki KAJITA¹, Katsuaki KASAHARA²,
and
Shoichi MIDORIKAWA³

¹ *Institute for Cosmic Ray Research, University of Tokyo, Tokyo 188*

² *Faculty of Engineering, Kanagawa University, Yokohama 221*

³ *Faculty of Engineering, Aomori University, Aomori 030*

(Received October 28, 2018)

The atmospheric neutrino-flux is calculated over the wide energy range from 1 GeV to 3,000 GeV for the study of neutrino-physics using the data from underground neutrino-detectors. The uncertainty of atmospheric neutrino-fluxes is also discussed. A brief comment is made to interpret the anomaly in terms of neutrino oscillations.

§1. Introduction

Since the observation of atmospheric neutrinos by the Kamiokande group¹⁾, some of the underground detectors^{2) 3)} have confirmed that the flux ratio of neutrino species $(\nu_\mu + \bar{\nu}_\mu)/(\nu_e + \bar{\nu}_e)$ is significantly different from the expected value, although the situation is still controversial^{4) 5)}. The atmospheric neutrino anomaly may have a crucial importance in particle physics, since it can be interpreted in terms of neutrino oscillations with a large mixing angle and a typical mass squared difference of $\mathcal{O}(10^{-2} \text{ eV}^2)$ ^{6) 7) 8) 9)}. The observation of the zenith angle variation of the double ratio $(\mu/e)_{data}/(\mu/e)_{MC}$ at multi-GeV energies is also suggestive¹⁰⁾. It is therefore important to calculate atmospheric neutrino fluxes precisely.

Atmospheric neutrino fluxes have been calculated from the incident beam of primary cosmic rays by Volkova¹¹⁾, Mitsui et al¹²⁾, Butkevich et al¹³⁾, and Lipari¹⁴⁾ mainly for high energies (from around 1 GeV to above 100,000 GeV). Gaisser et al¹⁵⁾, Barr et al¹⁶⁾, Bugaev and Naumov¹⁷⁾, Lee and Koh¹⁸⁾, and Honda et al¹⁹⁾ made a detailed calculation of the atmospheric neutrino fluxes for low energies from the primary cosmic rays. On the other hand, Perkins²⁰⁾ calculated the low energy atmospheric neutrinos using μ -flux observed at high altitude.

In this paper, we report the detailed calculation of the atmospheric neutrino fluxes in the energy range from 30 MeV up to 3,000 GeV, corresponding to the observation range of underground neutrino detectors²¹⁾. We also discuss the possibility to interpret the anomaly in terms of neutrino oscillations.

^{*)} Talk presented by S. Midorikawa, to appear in the Proceedings of Yukawa International Seminar '95: From the Standard Model to Grand Unified Theories.

§2. Primary Cosmic Ray Fluxes

Primary cosmic ray fluxes are relatively well known in the low energy region ($\lesssim 100\text{GeV}$), by which the low energy atmospheric ν -fluxes ($\lesssim 3\text{ GeV}$) are mainly produced. Webber and Lezniak²²⁾ have compiled the energy spectrum of the cosmic rays for the hydrogen, helium, and CNO nuclei in the range $10\text{ MeV} \sim 1,000\text{ GeV}$ for three levels of solar activity. A similar compilation has been made by others for hydrogen and helium nuclei, which agrees well with that of Webber and Lezniak.

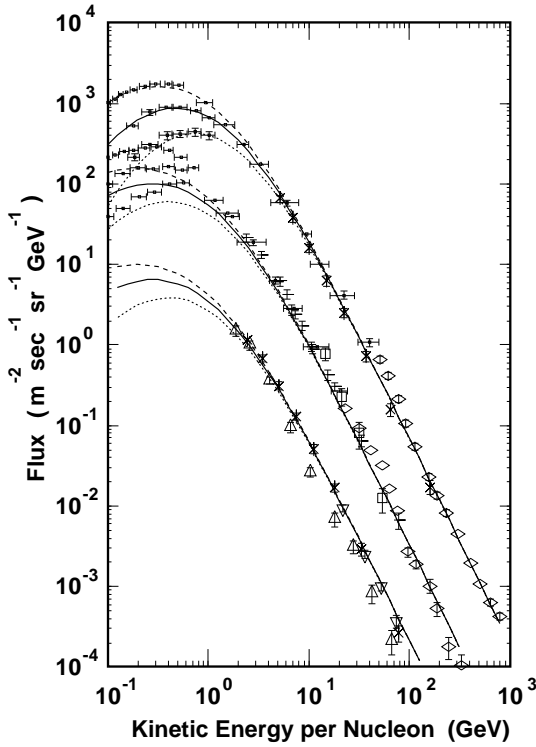


Fig. 1. Observed fluxes of cosmic ray protons, helium nuclei, and CNOs from the compilation of Webber and Lezniak¹⁾. Solid lines are our parametrization for solar mid, dashed lines for solar min., and dotted lines for solar max.

The geomagnetic field determines the minimum energy with which a cosmic ray can arrive at the earth. For the cosmic ray nucleus, the minimum energy of cosmic rays arriving at the earth is determined by the minimum rigidity (rigidity cutoff) rather than the minimum momentum. The value of the rigidity cutoff for the actual geomagnetic field can be obtained from a computer simulation of cosmic ray trajectories. If a cosmic ray particle can reach the earth, the antiparticle with an opposite momentum can escape from the earth. We launch antiprotons from the earth, varying the position and direction. When a test particle with a given momentum reaches a distance of 10 times of the earth's radius, it is assumed that the test particle has escaped from the geomagnetic field. The rigidity cutoff at Kamioka site is shown as the contour map in Fig. 2.

Cosmic rays with energy greater than 100 GeV , which are responsible for $\gtrsim 10\text{ GeV}$ atmospheric neutrino fluxes, are not affected by solar activity and by geomagnetic field. There are few measurements of the cosmic ray chemical composition at these energies, especially above 1 TeV . We compiled the available data and parametrized the observed fluxes for $\geq 100\text{ GeV}$ with a single power function, and show the result in table I. We treated bound nucleons at these energies as independent particles, and estimated the primary nucleon spectrum.

The geomagnetic field determines the minimum energy with which a cosmic ray can arrive at the earth. For the cosmic ray nucleus, the minimum energy of cosmic rays arriving at the earth is determined by the minimum rigidity (rigidity cutoff) rather than the minimum momentum. The value of the rigidity cutoff for the actual geomagnetic field can be obtained from a computer simulation of cosmic ray trajectories. If a cosmic ray particle can reach the earth, the antiparticle with an opposite momentum can escape from the earth. We launch antiprotons from the earth, varying the position and direction. When a test particle with a given momentum reaches a distance of 10 times of the earth's radius, it is assumed that the test particle has escaped from the geomagnetic field. The rigidity cutoff at Kamioka site is shown as the contour map in Fig. 2.

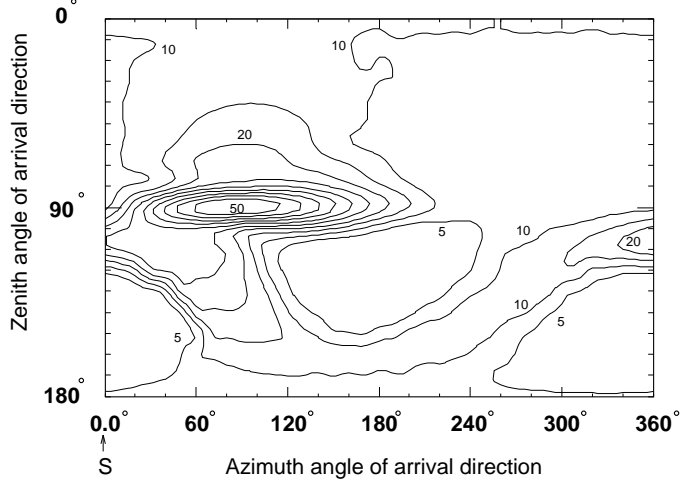


Fig. 2. The contour map of cutoff-rigidity for the ν arrival directions at Kamioka. Azimuthal angles of 0° , 90° , 180° , and 270° show directions of south, east, north, and west respectively.

Table I. Compiled cosmic ray spectrum in the form: $A(E/100 \text{ GeV})^\gamma$.

Nucleus	A	γ
H	$(6.65 \pm 0.13) \times 10^{-2}$	-2.75 ± 0.020
He	$(3.28 \pm 0.05) \times 10^{-3}$	-2.64 ± 0.014
CNO	$(1.40 \pm 0.07) \times 10^{-4}$	-2.50 ± 0.06
Ne-S	$(3.91 \pm 0.03) \times 10^{-5}$	-2.49 ± 0.04
Fe	$(1.27 \pm 0.11) \times 10^{-5}$	-2.56 ± 0.04

§3. Production and Decay of hadrons

As cosmic rays propagate in the atmosphere, they produce π 's and K 's in interactions with air nuclei. These mesons create atmospheric ν 's when they decay as follows:

$$\begin{aligned}
 A_{cr} + A_{air} &\rightarrow \pi^\pm, K^\pm, K^0, \dots \\
 \pi^+ &\rightarrow \mu^+ + \nu_\mu \\
 &\quad \mu^+ \rightarrow e^+ + \nu_e + \bar{\nu}_\mu \\
 \pi^- &\rightarrow \mu^- + \bar{\nu}_\mu \\
 &\quad \mu^- \rightarrow e^- + \bar{\nu}_e + \nu_\mu \\
 &\dots
 \end{aligned} \tag{3.1}$$

The calculations of the cosmic ray protons with air nuclei consists of a number of Monte Carlo codes corresponding to different primary energies. We employed the NUCRIN²³⁾ Monte Carlo code for the hadronic interaction of cosmic rays for $E_{lab} \leq 5 \text{ GeV}$, and LUND code – FRITIOF version 1.6²⁴⁾ and JETSET version 6.3²⁵⁾ – for $5 \text{ GeV} \leq E_{lab} \leq 500 \text{ GeV}$. Above 500 GeV, the original code developed by

Kasahara et al (COSMOS)²⁶⁾ was used. The K/π ratio is taken 7 % at 10 GeV, 11 % at 100 GeV, and 14 % at 1,000 GeV in laboratory energy.

We consider all the decay modes of π and K mesons but for rare ones. We have ignored charmed meson production, since the contribution of charmed particle to atmospheric neutrinos becomes sizable only for $E_\nu \gtrsim 100$ TeV.

In the two body decay of charged π 's and K 's, the resulting μ^\pm is fully polarized against (toward) the direction of μ motion in the charged π or K rest frame. We took into account the muon polarization effect in the subsequent decay following Hayakawa²⁷⁾. We applied the discussion in Ref. 28 for the polarization of μ 's from the $K_{3l\nu}$ decay. The small angle scattering of μ 's in the atmosphere reduces the μ polarization. This depolarization effect was also evaluated in Ref. 27 as of the order of $21 \text{ MeV}/vp$, where v and p are velocity and momentum of μ 's respectively.

§4. Atmospheric Neutrinos

At low energies, the rigidity cutoff has a significant directional variation. In the one-dimensional approximation which we adopted, we expect larger ν -fluxes from the low rigidity cutoff directions and a smaller ν -fluxes from the high rigidity cutoff direction. In the actual case, however, it may be difficult to observe these variations. There is a smearing effect of direction in the ν -detector. When a low energy ν ($\lesssim 3$ GeV) creates a charged lepton by a quasi-elastic process, the lepton has a typical angle of $50 - 60^\circ$ from the ν direction. Thus the directional dependence of atmospheric neutrino flux is small for lower energy neutrinos, especially when they are observed in the detector. We present in Fig. 3 the atmospheric neutrino fluxes averaging over all directions together with other calculations.

In Fig. 4, we show the flux ratio by ν -species along with those of other authors. Although the calculation method and some of physical assumptions are different among these authors, the ratio $(\nu_e + \bar{\nu}_e)/(\nu_\mu + \bar{\nu}_\mu)$ is very similar each other. The relatively large difference in $\bar{\nu}_e/\nu_e$ among them may reflect the difference of calculation scheme and/or the physical assumptions.

§5. Uncertainties

The systematic error in the calculation of atmospheric ν -fluxes comes mainly from the incompleteness of the knowledge of the primary cosmic ray fluxes. Even at low energies, where the primary cosmic ray fluxes are rather well studied, it is difficult to determine the absolute value due to the uncertainties in the instrumental efficiency ($\sim 12\%$) and exposure factor ($2 - 3\%$). In our compilation, the error in the fit is $\sim 10\%$ for the nucleon flux at 100 GeV and $\sim 20\%$ at 100 TeV. Assuming $\sim 10\%$ uncertainty below 100 GeV, the systematic error in the atmospheric ν -fluxes is estimated to be $\sim 10\%$ at ≤ 3 GeV, increasing to $\sim 20\%$ at 100 GeV, and remains almost constant up to 1,000 GeV.

The interaction model is another source of systematic errors. In our comparison, the agreement of the LUND model and the COSMOS code with the experimental data is $\lesssim 10\%$. The authors of the NUCRIN code claim that the agreement is within

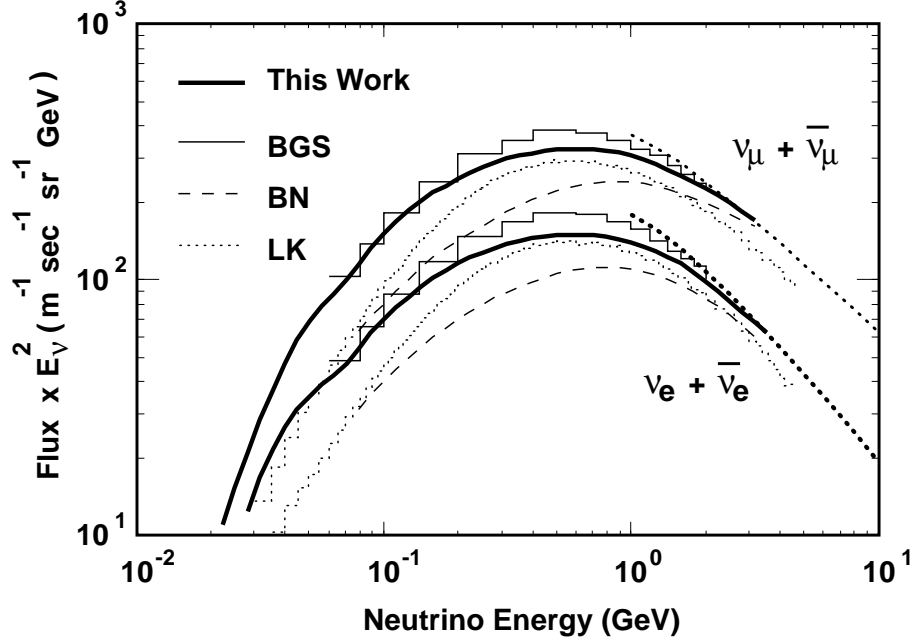


Fig. 3. The atmospheric ν -fluxes multiplied by E_ν^2 for the Kamioka site at solar mid. (solid line). BGS are from Ref. [16], BN from Ref. [17], and LK from Ref. [18]. The dotted line is the result from the calculation for high energy without the rigidity cutoff, and averaged over all directions.

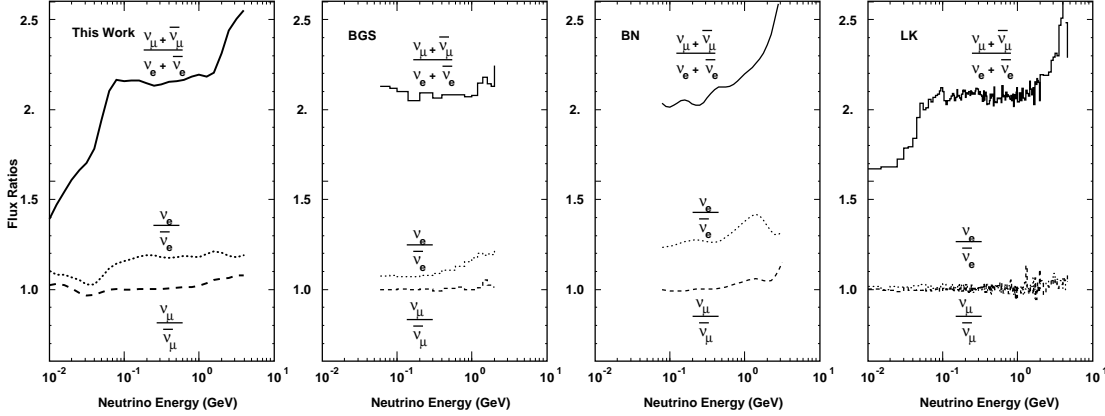


Fig. 4. The flux ratio of ν -species calculated for Kamioka. BGS are from Ref. [16], BN from Ref. [17], and LK from Ref. [18] as before.

10 – 20 %²³). The hadronic interaction below 5 GeV contributes at most 5 % to the production of atmospheric ν -fluxes at 1 GeV. The systematic error caused by the hadronic interaction model is estimated to be ~ 10 % above 1 GeV.

One-dimensional approximation which we have adopted is justified only at high energies. It is expected to be accurate above 3 GeV. Since the calculation of rigidity cutoff is very simplified in this scheme, this may result in a systematic error in the

absolute value of the atmospheric neutrino fluxes of 10 – 20 % at 100 MeV and 5 % at 1 GeV.

The statistics of the Monte Carlo calculation also causes an error in the atmospheric neutrino fluxes. The uncertainty due to the statistics is estimated to be $\lesssim 5\%$ up to 100 – 300 GeV for ν_μ and $\bar{\nu}_\mu$, and up to 30 – 100 GeV for ν_e and $\bar{\nu}_e$, depending on the zenith angle. The errors increase to $\sim 10\%$ at the highest energy for each kind of ν 's.

Combining all the systematic and non-systematic errors, the total error is estimated as 15 % from 1 GeV to 100 GeV, and 20 – 25 % at the highest energy in our calculation. However, the error of the species ratio is smaller than that of the absolute value, since the ν -species ratio is not affected much by the uncertainty of primary fluxes and the calculation scheme. It is estimated to be $\lesssim 10\%$ below 100 GeV for $\nu/\bar{\nu}$ and $\lesssim 5\%$ below 30 GeV for $(\nu_\mu + \bar{\nu}_\mu)/(\nu_e + \bar{\nu}_e)$. These errors also increase to 10 – 15 % at the highest energies in our calculation.

§6. Neutrino Oscillations

We compare the Kamiokande data¹⁰⁾ with the theoretical calculations. As in our previous paper⁸⁾, we define,

$$\langle \varepsilon_\alpha \sigma_\alpha F_\beta \rangle = \sum_{\nu, \bar{\nu}} \int \varepsilon_\alpha(E_\alpha) \sigma_\alpha(E_\nu, E_\alpha) F_\beta(E_\nu, \Omega_\nu) \rho(h) dE_\alpha dE_\nu d\Omega_\nu dh, \quad (6.1)$$

where $\varepsilon_\alpha(E_\alpha)$ is the detection efficiency for an α -type charged lepton with energy E_α , σ_α the differential cross section of ν_α , $F_\beta(E_\nu, \Omega_\nu)$ the incident ν_β flux with energy E_ν and zenith angle Ω_ν .

Instead of the number N_e^{obs} and N_μ^{obs} of the observed electron and muon events, we use the ratios defined as follows:

$$f_1 = \frac{\langle \varepsilon_\mu \sigma_\mu F_e \rangle}{\langle \varepsilon_\mu \sigma_\mu F_\mu \rangle}, \quad f_2 = \frac{\langle \varepsilon_e \sigma_e F_e \rangle}{\langle \varepsilon_e \sigma_e F_\mu \rangle}, \quad (6.2)$$

and

$$U_e = \frac{N_e^{obs}}{\kappa \langle \varepsilon_e \sigma_e F_\mu \rangle} = f_2 \frac{N_e^{obs}}{N_e^{MC}} \quad (6.3)$$

$$U_\mu = \frac{N_\mu^{obs}}{\kappa \langle \varepsilon_\mu \sigma_\mu F_\mu \rangle} = \frac{N_\mu^{obs}}{N_\mu^{MC}}, \quad (6.4)$$

where ($\kappa = [\text{number of nucleons}] \times [\text{time}]$), N_e^{MC} and N_μ^{MC} are the expected numbers of electron and muon events from the Monte Carlo calculations respectively.

If there is no ‘atmospheric neutrino anomaly’, the data would point to $(f_2, 1)$ in the (U_e, U_μ) plain. Note that the effects of flux models, geomagnetic cutoffs, and the detection efficiencies are all included in the values of f_1 and f_2 . We find $f_1 \simeq f_2 \simeq 0.473 = f$ from our neutrino fluxes and the detection efficiency of the sub-GeV data at Kamiokande.

If there are neutrino oscillations, the ratios U_e and U_μ become

$$U_e = f_2 \langle P(\nu_e \rightarrow \nu_e) \rangle + \langle P(\nu_\mu \rightarrow \nu_e) \rangle \quad (6.5)$$

$$U_\mu = \langle P(\nu_\mu \rightarrow \nu_\mu) \rangle + f_1 \langle P(\nu_e \rightarrow \nu_\mu) \rangle, \quad (6.6)$$

where the bracket means the average over the distances and energies of neutrinos:

$$\langle P(\nu_\beta \rightarrow \nu_\alpha) \rangle = \frac{1}{\kappa \langle \varepsilon_\alpha \sigma_\alpha F_\beta \rangle} \times \sum_{\nu, \bar{\nu}} \int \varepsilon_\alpha(E_\alpha) \sigma_\alpha(E_\nu, E_\alpha) F_\beta(E_\nu, \Omega_\nu) P(\nu_\beta \rightarrow \nu_\alpha) \rho(h) dE_\alpha dE_\nu d\Omega_\nu dh. \quad (6.7)$$

Table II. the values of U_e , U_μ , and U_e/U_μ calculated from both the sub- and multi-GeV data for the Kamioka site with an exposure of $7.7 \text{ ktn} \cdot \text{yr}$. The value f is taken to be $f = 0.473$.

Energy	U_e	U_μ	U_e/U_μ
Sub-GeV	0.518 ± 0.084	0.656 ± 0.103	0.790 ± 0.072
Multi-GeV	0.697 ± 0.126	0.832 ± 0.144	0.838 ± 0.111

We summarize in Table II the values of U_e , U_μ , and U_e/U_μ which are obtained from both the sub- and multi-GeV data with $7.7 \text{ ktn} \cdot \text{yr}$. We used only single ring events for the analysis of sub-GeV data. For the multi-GeV data, we used both single and multi ring events, and evaluated U_e using Eq. 6.4 with $f_2 = f$ obtained from the sub-GeV data so that we can compare both data directly. We combine the statistical and systematic errors of $\sim 15\%$ including the uncertainty in the neutrino cross section.

We show in Fig. 5 the regions allowed by the Table II together with the region (U_e, U_μ) allowed by three neutrino oscillations assuming $f_1 = f_2 \equiv f$.

From this figure, we find that the sub-GeV and multi-GeV data are marginally consistent each other, and that it is possible to explain the anomaly in terms of three neutrino oscillations. Although it may be premature to deduce what mode dominates oscillations, the multi-GeV data seem to suggest $\nu_e \longleftrightarrow \nu_\mu$ oscillations, while the sub-GeV data prefer $\nu_\mu \longleftrightarrow \nu_\tau$ oscillations. It seems that U_e and U_μ grow with energy, keeping the U_μ/U_e ratio almost constant. The same conclusion has also been drawn by Fogli and Lisi²⁹⁾. This effect may be explained by the improvement of the data and/or calculations. However, if we take both the theory and the experiment seriously, we are led to a more fascinating conjecture. We can explain both data if matter enhanced oscillations would occur between sub- and multi-GeV regions.

In conclusion, we have shown a detailed calculation of atmospheric neutrinos and a new analysis of the anomaly using the recent Kamiokande data. The atmospheric neutrino anomaly is eager for further confirmation by another types of neutrino experiments such as a long baseline experiment.

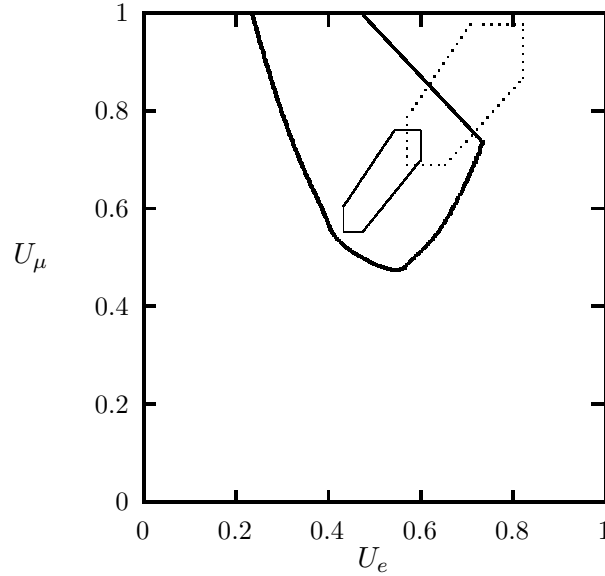


Fig. 5. Analysis of the Kamiokande data. Bold line : Allowed region by three neutrino oscillations. Solid line: Kamikande Sub-GeV data. Dashed line: Kamiokande Multi-GeV data.

Acknowledgements

This work is supported in part by Grant-in-Aid for Scientific Research, of the Ministry of Education, Science and Culture #07640419.

References

- [1] K.S. Hirata et al, Phys. Lett. B **205**, 416 (1988).
- [2] D. Casper et al, Phys. Rev. Lett. **66**, 2561 (1991); R. Becker-Szendy et al, Phys. Rev. D **66**, 2561 (1991).
- [3] T. Kafka, Nucl. Phys. B (Proc. Suppl.) **35**, 427 (1994).
- [4] Ch. Berger et al, Phys. Lett. B **227**, 489 (1989); **245** 305 (1990).
- [5] M. Aglietta, et al, Europhys. Lett. **8**, 611 (1989).
- [6] J.G. Learned, S. Pakvasa, and T.J. Weiler, Phys. Lett. B **207**, 79 (1988).
- [7] V. Berger and K. Whisnant, Phys. Lett. B **209**, 365 (1988).
- [8] K. Hidaka, M. Honda, and S. Midorikawa, Phys. Rev. Lett. **61**, 1537 (1988); S. Midorikawa, M. Honda, and K. Kasahara, Phys. Rev. D **44**, 3379 (1991).
- [9] K.S. Hirata et al, Phys. Lett. B **280**, 146 (1992).
- [10] Y. Fukuda, et al, Phys. Lett. B **335**, 237 (1994).
- [11] L.V. Volkova, Yad. Fiz. **31**, 1510 (1980) [Soviet J. Nucl. Phys. **37**, 784 (1980)].
- [12] K. Mitsui, Y. Minorikawa, and H. Komori, Nuovo Cimento **9C**, 995 (1986).
- [13] A.V. Butkevich, L.G. Dedenko, and I.M. Zhelsnykh, Yad. Fiz. **50**, 142 (1989) [Soviet J. Nucl. Phys. **50**, 90 (1989)].
- [14] P. Lipari, Astroparticle Phys. **1**, 195 (1993).
- [15] T.K. Gaisser, T. Stanev, and G. Barr, Phys. Rev. D **38**, 85 (1988).
- [16] G. Barr, T.K. Gaisser, and T. Stanev, Phys. Rev. D **39**, 3532 (1989).
- [17] E.V. Bugaev and V.A. Naumov, Phys. Lett. B **232**, 391 (1989).
- [18] H. Lee and Y. Koh, Nuovo Cimento B **105**, 884 (1990).
- [19] M. Honda, K. Kasahara, K. Hidaka, and S. Midorikawa, Phys. Lett. B **248**, 193 (1990).
- [20] D.H. Perkins, Astroparticle Phys. **2**, 249 (1990).
- [21] M. Honda, T. Kajita, K. Kasahara, and S. Midorikawa, ICRR-Report-336-95-2 (1995), to

- be published in Phys. Rev. D.
- [22] W.R. Webber and J.A. Lezniak, *Astrophys. Space Sci.*, **30**, 361 (1974).
 - [23] K. Hänssget and J. Ranft, *Comput. Phys.*, **39**, 37 (1986); *Nucl. Sci. Eng.*, **88**, 537 and 551 (1984).
 - [24] B. Nilsson-Almqvist and E. Stenlund, *Comput. Commun.* **43** 387 (1987).
 - [25] Sjöstrand T. et al., *Comput. Commun.* **43**, 367 (1987).
 - [26] K. Kasahara, and S. Torii, *Comput. Phys. Commun.* **64**, 109 (1991); K. Kasahara, S. Torii, and T. Yuda, in *Proceedings of the 16th ICRC, Kyoto 1979* (University of Tokyo, Tokyo, Japan, 1979) Vol. 13, p. 70.
 - [27] S. Hayakawa, *Phys. Rev.* **108**, 1533 (1957).
 - [28] N. Brene, L. Egrade, and B. Qvist, *Nucl. Phys.* **22**, 553 (1961).
 - [29] G.L. Fogli and E. Lisi, *Phys. Rev. D* **52**, 2775 (1995).